minerals

MDPI

Article

Optimization of Ni(II), Pb(II), and Zn(II) Ion Adsorption Conditions on Pliocene Clays from Post-Mining Waste

Beata Jabłońska

Faculty of Infrastructure and Environment, Czestochowa University of Technology, Brzeźnicka St. 60a, 42-200 Częstochowa, Poland; beata.jablonska@pcz.pl

Abstract: Lignite mining results in a significant amount of waste clayey materials—the so-called Pliocene clays, which are often considered useless mineral waste. One method of management is to use them as inexpensive adsorbents in water and wastewater treatment, or as permeable barriers in groundwater remediation. The study is an attempt to use the raw Pliocene clays to remove Pb(II), Ni(II), and Zn(II) ions from wastewaters. The mineralogical composition, physicochemical, granulometric, structural, and surface properties were examined. The value of the point of zero charge pH of the adsorbent was found to be 7.1. To determine the optimal adsorption conditions, the central composite design (CCD) method was used with the pH of the solution, metal ion concentration, and the adsorbent mass as independent variables, and the percentage removal as the response variable. The determined optimal values of the adsorbent mass and the solution pH turned out to be similar for all three metals, with a pH of 6–7 and an adsorbent dose of 18–24 g/dm^3. In further tests, the pH was established slightly lower than it would appear from the CCD method in order to avoid the possible precipitation of metals in the form of hydroxides. The kinetics of sorption were investigated and it was found that the sorption process ran for several minutes. The effect of temperature showed that the adsorption was spontaneous and thermodynamically favored. The leachability of the metals indicated that Pb(II) and Zn(II) were strongly bound in the adsorbent, whereas Ni(II) manifested a larger mobility. It was found that the tested clays had quite good sorption properties in relation to the tested metal ions and could be used for water and wastewater treatment.

Keywords: adsorption; beidellite clays; heavy metals; mining waste

check for updates

Citation: Jabłońska, B. Optimization of Ni(II), Pb(II), and Zn(II) Ion Adsorption Conditions on Pliocene Clays from Post-Mining Waste. *Minerals* **2021**, *11*, 568. https://doi.org/10.3390/min11060568

Academic Editor: Dorota Kołodyńska

Received: 6 April 2021
Accepted: 24 May 2021
Published: 26 May 2021

Publisher's Note: MDPI stays neutral with regard to jurisdictional claims in published maps and institutional affiliations.

Copyright: © 2021 by the author. Licensee MDPI, Basel, Switzerland. This article is an open access article distributed under the terms and conditions of the Creative Commons Attribution (CC BY) license (https://creativecommons.org/licenses/by/4.0/).

1. Introduction

Opencast mining results in a significant amount of post-mining waste. According to the Central Statistical Office [1], the main source of waste in Poland in 2019 was, as in previous years, mining and extraction (55.8% of the total amount of generated waste). Nearly 5.3 Mt of waste were generated in Poland in the extraction of minerals other than metal ores in 2019, while the amount of this waste that accumulated on heaps in mines was 96.8 Mt [1]. Although the amount of mining waste has decreased compared with previous years, the amount of waste that accumulated in heaps and was not used has not lowered significantly. It is estimated that lignite opencast mining in the Bełchatów mine requires the annual removal of 110 to 130 million m^3 of accompanying mineral overburden [2]. Among these are the so-called Pliocene clays. The data on the amount of exploited and deposited clays in the Bełchatów mine are not clear. According to [3], the mine exploited 1.03 Mt of clay up until 2015, and up to 100 thousand m^3 of clay arises each year. Considerable resources, as well as the fact that they are deposited in the mineral landfills accompanying the main mineral extraction (the so-called secondary deposits), facilitate their management. The deposits of clayey minerals have been studied and documented mainly for precious and construction ceramics [4,5], for the production of ceramized fertilizer composites, or expanded clay [6]. There have also been attempts to use the clays in adsorption processes [7–9]. The prevalence of clay waste from lignite opencast

mines and the possibility of using them directly or after very simple processing were reasons for undertaking the research into determining their suitability for environmental protection purposes.

Human activities, such as industrialization and urbanization, contribute largely to the increasing pollution of soil and water with various heavy metals. Many of them do not play any role in the process of cell metabolism, but are easily absorbed and accumulated in various parts of plants and other living organisms [10,11]. Examples are lead and nickel [12,13]; in addition zinc, although required in small amounts [14], is harmful in larger concentrations. In plants, zinc and nickel in excessive concentrations (100–400 $mg \cdot kg^{-1}$, depending on the species) cause the development of chlorosis and necrosis. This phenomenon is associated with iron deficiency and the inhibition of photosynthesis [15]. Lead also contributes to the inhibition of photosynthesis in plants, and slows down the rate of fat conversion and water absorption in plants. The presence of unbound lead in the tissue causes severe disturbances in metabolism, as it limits the activity of enzymes, especially those that are involved in fat metabolism, and also blocks the synthesis of hemoglobin [14]. The excess of nickel in living organisms is easily bioaccumulated and causes damage to the mucous membranes. In addition, the toxic effect of nickel on the body is manifested by allergic reactions, disturbances in plasma protein metabolism, and changes in the chromosomes and bone marrow [11].

The contamination of water with heavy metals is of particular importance because of the role water plays in the circulation of chemical components between various elements of the environment. The main sources of pollution of the aquatic environment are emissions of toxic substances from industrial plants, leachate from landfills, pipelines, and surface runoff from communication routes and agricultural areas. Most often, the discharge of municipal, industrial, and mine wastewater is local; therefore, in the vicinity of its runoff, a significant increase in trace elements, including heavy metals, is usually observed in the water–soil environment [11,16]. Some of the pollutants from such wastewater may migrate over long distances and also to greater depths, thus contributing to the contamination of deep waters [11]. The extraction of metal ores also contributes to the generation of large amounts of waste and sewage containing various metal compounds, which accumulate in the environment over time [17]. The mining and processing activities of non-ferrous metals are sources of increased concentrations of Ni(II), Pb(II), and Zn(II) ions in the environment [18]. These metals occur locally in surface- and ground-water as a result of the infiltration of polluted waters from ponds in which flotation waste is deposited, e.g., formed in the process of mechanical enrichment of Zn and Pb ores [19], as well leachates from industrial waste landfills out of operation, which pose a serious threat to the natural environment [20–22]. The accumulation of metals in the soil increases over time, and is not only the result of mining activities, but is also influenced by metal-containing minerals, geographical features, and the local dominant wind in the area [23]. Currently, China is the world's largest center for the production and consumption of zinc and lead. In recent years, a significant increase in demand has also occurred in the United States [24]. The global extraction of nickel, lead, and zinc by mines in 2019 was 2.61, 4.72, and 12.7 Mt, respectively [25]. In 2019 in Poland, the extraction of zinc and lead ores amounted to 1.51 Mt of ore, containing 40 kt of zinc and 20 kt of lead [26].

In the processes of the leaching and migration of heavy metals, sorption by solid phase in the pores in which aqueous solutions circulate plays a special role. In sorption processes in water and wastewater treatment, synthetic substances are usually used as adsorbents, e.g., activated carbon [27], ion exchange resins [28], and zeolites [29]. Their disadvantage is the significant production costs; therefore, low-cost sorbents that could be used in wastewater treatment or pre-treatment are constantly searched for [30–32]. Immobilization of heavy metals in wastewater can also be carried out with the use of natural aluminosilicate minerals, which include, inter alia, montmorillonite, zeolite, kaolinite, illite, vermiculite, and chlorite. Aluminosilicate minerals have very good cation exchange abilities. They are active because of their large specific surface, which, depending on the mineral, ranges

from a dozen to even 700–800 m^2/g [33]. The effective sorption of heavy metals by clayey raw minerals may be the first step in neutralizing heavy metal ions. The next step to the permanent neutralization of these contaminants may be the ceramization of the material used in adsorption in order to even more permanently immobilize heavy metal cations [34,35].

So far, the sorption properties of most mineral wastes have been poorly explored in relation to various types of harmful substances, including heavy metals, originating from extensive or point pollution sites. Meanwhile, because of the specific composition of solid waste, some of them may have better retention properties for toxic components than typical soils of the aeration zone. This makes it possible to use mineral waste materials with appropriate properties as filling protective barriers against the threat to the aquatic environment from point and extensive pollution foci, e.g., dumps. The use of the waste clays considered here for adsorption has been investigated in previous works [7–9]. These studies focused mainly on the characterization of the material and the adsorption of selected substances on raw and chemically or thermally modified clays from different locations for previously selected conditions. As chemical or thermal modifications require additional procedures and financial outlays, the aim of this work was to determine the optimal conditions for the adsorption of selected heavy metals on natural Pliocene clays. The paper discusses the results of the research on the use of waste raw clayey materials from Pliocene clays from lignite mining in the sorption process for the removal of Zn(II), Pb(II), and Ni(II) in wastewater treatment or as permeable barriers in groundwater remediation. Among others, the central composite design (CCD) for the adsorbent dose, solution pH, and ion concentration was used to determine the best conditions for the removal of the heavy metals considered here. The kinetics of the sorption were also investigated, and the leaching aspects were also discussed.

2. Materials and Methods

2.1. Materials

The clay samples were taken from the Bełchatów lignite opencast mine from the Szczerców field. The Bełchatów mine (central Poland) exploits the lignite deposit located within the Mesozoic formations in the tectonic ditch of a complicated geological structure extending in the W-E direction [3]. It is about 6.5 km long and 1–2.5 km wide. It arose from a syngenetic tectonic depression. The overburden rocks belong to the Neogene sediments. The main clayey mineral in the lignite overburden is classified as beidellite clay from the Pliocene clay-sand horizons of the Polish Lowlands. The samples were acquired from the dump where overburden is selectively stored as a raw waste mineral. The studied clays (Figure 1a) were dried to an air-dry state at a temperature of 105 °C, and were comminuted to a grain size below 0.1 mm (Figure 1b).



(**a**) (**b**)

Figure 1. (**a**) Raw and (**b**) comminuted Pliocene clay.

2.2. Instruments

The mineralogical composition was determined by XRD analysis on a D8 Advance X-ray diffractometer with a CuKα and ultrafast LynxEye semiconductor detector (Bruker, Billerica, MA, USA). The tests were conducted at room temperature. The mineralogical composition was also investigated via thermal method using a TGA/SDTA 851e thermogravimeter (Mettler Toledo, Greifensee, Switzerland). The TG/DTG/DTA analyses were performed by heating 10 mg of the sample in air to 1000 °C at a heating rate of 10 °C/min. The particle size analysis was performed on an Analysette 22 NeXT (Fritsch, Idar-Oberstein, Germany). The specific surface area and pore volume were determined by the adsorption/desorption of liquid nitrogen on an AutosorbiQ volumetric analyzer (Quantachrome Instruments, Boynton Beach, FL, USA). Low-temperature (−196 °C) nitrogen adsorption/desorption isotherms were determined in the range of relative pressures from about 0.01 to 0.995. Before the measurements, the samples were degassed at a temperature of 150 °C for 6 h under a pressure of 10^{-4} mmHg. The chemical composition was determined by wavelength dispersive X-ray fluorescence spectrometry (WD-XRF) using an ADVANT XP sequential spectrometer (Thermo ARL, Waltham, MA, USA). The concentration of metal ions in water extracts and samples after sorption was analyzed using an atomic emission spectrometer with inductively coupled plasma of the ICP-AES type. The pH measurements were carried out with a pH/mv CP-401 pH meter (ELMETRON, Zabrze, Poland) with an accuracy of +/− 0.002 pH.

2.3. Methods

2.3.1. Physical and Chemical Analyses

The analyses of the individual physical and chemical properties of the Pliocene clays were performed in accordance with the applicable standards. The chemical composition of the tested samples was performed using the XRF spectral method described in [36]. The contents of the non-flammable parts (ash) and flammable parts (losses on ignition) were determined according to [37]. When determining the flammable and non-flammable components, the samples were calcined at a temperature of 815 °C to a constant weight in an FCF22S muffle furnace (Czylok, Jastrzębie-Zdrój, Poland). The tests for the leaching pollutants from the waste were carried out for a ratio of liquid to solid phase equal to 10 dm^3/kg, in accordance with the standard [38]. The content of heavy metals in the samples after the sorption process was determined using the ICP-AES spectrometer.

2.3.2. Point of Zero Charge

The point of zero charge pH (pH_{pzc}) of the clay samples was determined according to [39], using the constant addition method, where 50 mL of 0.01 mol/dm^3 NaCl solution was prepared in polyethylene bottles. These solutions were adjusted to a pH from 2 to 11 and were left for 2 h. After this time, the initial pH of the solution was determined ($pH_{initial}$), and then 0.15 g of the adsorbent was added to each bottle. Each sample was flushed with nitrogen gas and was plugged. Then, the samples were shaken for 24 h and allowed to stand for 24 h. After 48 h of equilibration, the final pH (pH_{final}) was measured. The pH_{pzc} value was determined from the plot ($pH_{initial}$-pH_{final}) vs. $pH_{initial}$.

2.3.3. Sorption Tests

The studies on the sorption of Ni(II), Pb(II), and Zn(II) ions on the Pliocene clays were carried out using the static batch method from synthetic solutions of metal nitrates. The flask samples prepared in this way were shaken in a shaking water bath (357 ELPINA+). After adjusting the temperature, the samples were shaken for 2 h, and then remained static for another 22 h. In the next step, the water from the conical flasks was decanted and centrifuged on a centrifuge (MPW-223, MPW, Warsaw, Poland) at a speed of 2500 rpm in order to remove the clay material from the solution. The concentration of metal ions in the obtained eluates was analyzed using an ICP-AES spectrometer.

The thermodynamic and kinetics of the sorption of heavy metals (initial concentration of 100 mg/dm^3 and 200 mg/dm^3) were carried out in suspensions of minerals at a concentration of 2%. The tests in the thermodynamic studies were carried out at temperatures ranging from 20 °C to 50 °C. In the kinetics analyses, times from 5 min to 360 min were applied as the contact time of the sorbent with the aqueous solution.

For each sample, three series of measurements were performed, and the test results included the average values. The amount of absorbed metal, q (mg/g), was calculated as follows:

$$q = \frac{C_0 - C_e}{m} V, \quad (1)$$

where C_0 and C_e are the initial and equilibrium concentration of metal ions (mg/dm^3), respectively; V is the volume of the solution (dm^3); and m is adsorbent mass in the volume (g).

2.3.4. Optimization of Adsorption Conditions

The central composite design (CCD) approach was used in the research to determine the optimal conditions for Zn(II), Pb(II), and Ni(II) removal from aqueous solutions with the use of adsorption on Pliocene clays. The independent variables were the initial pH of the solution(pH$_0$), initial concentration of metal ions (C_0, mg/dm^3), and adsorbent mass per solution mass (m, g). The response variable was the metal removal, R (%), calculated as follows:

$$R = \frac{C_0 - C_e}{C_0} 100\%, \quad (2)$$

where C_e (mg/dm^3) is the equilibrium concentrations of the metal ions. The ranges of the independent variables were 3 to 7 for pH$_0$, 10 to 90 mg/dm^3 for the Zn(II) and Ni(II) initial concentration, 100 to 300 mg/dm^3 for the Pb(II) initial concentration, and 1 to 5 g for the mass adsorbent at a solution volume 200 cm^3. The pH of the solutions was adjusted using 0.1 M NaOH or 0.1 M HCl solutions. The samples were shaken for 2 h, and then the flasks were placed in at a room temperature of 20 °C for 22 h (total contact time with the adsorbent was 24 h).

According to the standard CCD for three independent variables (CCD3), a total of 20 measurement points were used for each measurement series. First, the independent variables pH$_0$, C_0, and m were coded and denoted as x_1, x_2, and x_3, respectively. Each coded variable was tested for five levels, equal to the following $-\alpha$, -1, 0, 1, α, where $\alpha = 2^{3/4} \approx 1.682$. The values of $-\alpha$ and α correspond to the minimum and maximum value of the independent variables, respectively, as follows:

$$\mathrm{pH}_0 = \frac{\mathrm{pH}_{0,\max} + \mathrm{pH}_{0,\min}}{2} + \frac{\mathrm{pH}_{0,\max} - \mathrm{pH}_{0,\min}}{2\alpha} x_1 \quad (3)$$

Similar expressions are used for the two remaining variables (C_0 and m). The CCD3 design allows for performing much less measurements for more levels of independent variable values (20 points and 5 levels) than in the case of the full factorial analysis (27 points, 3 levels), keeping the accuracy as high as possible.

According to the CCD3 procedure, the response value is described via a second order polynomial of x_1, x_2, and x_3, i.e.,

$$\widetilde{R} = a_0 + a_1 x_1 + a_2 x_2 + a_3 x_3 + a_4 x_1 x_2 + a_5 x_1 x_3 + a_6 x_2 x_3 + a_7 x_1^2 + a_8 x_2^2 + a_9 x_3^2, \quad (4)$$

where $\widetilde{R}$ is the predicted removal, a_0 and, $a_1, \ldots, a_9$ are the coefficients determined via the least squares method based on the measurements. To reduce the number of terms, a series of analyses were performed with all of the possible subsets of terms, and the adjusted coefficient of determination, R^2, was used to select the best fit. In contrast with R^2, the adjusted R^2 penalizes the number of terms if they do not considerably improve the fitness quality. The analysis was performed in Mathematica.

2.3.5. Adsorption Kinetics

Theoretical studies on the adsorption kinetics were carried out using the most commonly used models, namely: pseudo-first order, pseudo-second order, and intraparticle diffusion [40].

In the Lagergren's pseudo-first order (PFO) model, it is assumed that the adsorption rate is proportional to the number of free adsorption sites. This, in turn, is proportional to the difference between the amount of substance adsorbed at equilibrium, q_e (mg/g), and the amount of substance adsorbed so far, $q(t)$ (mg/g):

$$\frac{dq}{dt} = k_1(q_e - q) \tag{5}$$

where the proportionality coefficient k_1 (1/min) determines the adsorption rate. A simple integration yields the following

$$q(t) = q_e\left(1 - e^{-k_1 t}\right) \tag{6}$$

According to this model, the time of half-saturation, when q reaches $0.5q_e$, equals the following

$$t_{1/2} = \frac{\ln 2}{k_1} \tag{7}$$

The Lagergren model is based on one-site adsorption, and often does not reflect the actual adsorption process very well. A generalization was proposed by involving a two-site adsorption, described by the following equation:

$$\frac{dq}{dt} = k_2(q_e - q)^2 \tag{8}$$

where k_2 (g/(mg·min)) reflects the speed of the process. In the integral form one gets

$$q(t) = q_e \frac{q_e k_2 t}{1 + q_e k_2 t} \tag{9}$$

This model is referred to as a pseudo-second order (PSO). The half-saturation time equals

$$t_{1/2} = \frac{1}{k_2 q_e} \tag{10}$$

The intraparticle diffusion (IPD) is based on the diffusion process. Considering the process of diffusion of the adsorbate of constant concentration into spherical particles, the following expression is obtained

$$q(t) = q_e\left(1 - \frac{6}{\pi^2}\sum_{n=1}^{\infty}\frac{1}{n^2}\exp\left(-\frac{n^2\pi^2 Dt}{r^2}\right)\right) \tag{11}$$

where r is the radius of the adsorbent particles and D (m^2/min) is the diffusion coefficient. For calculation purposes, this series is approximated by the expression as follows:

$$q(t) = k_i\sqrt{t} + C \tag{12}$$

where k_i (mg/(g·$min^{1/2}$)) is a substitutive coefficient characterizing the diffusion process. In the initial stage of diffusion, the equivalent thickness of the adsorption layer is proportional to the square root of time, and then the value of constant C (mg/g) equals zero, and the value of k_i can be expressed as follows:

$$k_i|_{C=0} = \frac{6q_e}{r}\sqrt{\frac{D}{\pi}} \tag{13}$$

With the passage of time, the adsorbent is gradually saturated, which finds a reflection in an increase in the value of C, and then Equation (13) does not apply. The half-saturation time for Equation (11) equals

$$t_{1/2} \approx \frac{0.03r^2}{D} \tag{14}$$

If the adsorption time is long enough, only the lowest-order term (n = 1) can be retained in Equation (11), yielding an expression similar to that for PFO:

$$q(t) = q_e\left(1 - \frac{6}{\pi^2}\exp(-Bt)\right) \tag{15}$$

where $B = \pi^2 D/r^2$. This model will be referred as to IPD1. Unlike PFO, the IPD1 model allows for estimating the value of D if the radius of the adsorbent particles, r, is known:

$$D = \frac{Br^2}{\pi^2} \tag{16}$$

Because of the fact that the PFO and IPD1 models cannot be fully linearized, the coefficients k_1, k_2, k_i, q_e, B, and C were determined using nonlinear regression for Equations (6), (9), (12), and (15). As the coefficient of determination R^2 is not an adequate measure of fit quality in nonlinear regression, the standard error of regression S and χ^2 values, defined as follows, were used:

$$\chi^2 = \sum_{i=1}^{n} \frac{(q_i - q(t_i))^2}{q(t_i)} \tag{17}$$

where n is the number of measurement points, q_i is the measured values, and $q(t_i)$ is the values predicted by the model. In turn, the standard error of regression S equals

$$S = \sqrt{\frac{1}{n-p-1}\sum_{i=1}^{n}(q_i - q(t_i))^2} \tag{18}$$

where p = 2 is the number of parameters in each model. The values of the explained variable with a probability of 95% are located not further than 2S from the regression line.

2.3.6. Thermodynamic Studies

To assess the thermodynamic parameters related to the adsorption process, the Van't Hoff equation was used in the following form:

$$\ln K_e = \frac{\Delta S}{R} - \frac{\Delta H}{RT} \tag{19}$$

where

$$K_e = \frac{C_{Ae}}{C_e} \tag{20}$$

is the equilibrium constant, C_e (mg/dm^3) is the equilibrium concentration of metal ions, C_{Ae} (mg/dm^3) is the equilibrium concentration of the adsorbent, ΔS (J/(mol K)) is the entropy change, ΔH (kJ/mol) is the enthalpy change, T (K) is the temperature, and $R \approx 8.314$ J/(mol K) is the gas constant. The parameters ΔS and ΔH were assumed to be constant in the considered temperature range of 20 to 50 °C, and were determined by linear fitting of $\ln K_e$ vs. $1/T$. The Gibb's free energy was assessed as follows:

$$\Delta G = \Delta H - T\Delta S = -RT \ln K_e \tag{21}$$

2.3.7. Leaching Studies

The study of the leachability of metals after sorption was carried out in accordance with the Polish standard [38]. The tested material after adsorption (initial concentration of

each metal was 100 mg/dm^3) was added to water at a ratio of 1:10 (dry mass of waste to the mass of water). After shaking and sedimentation, the water was decanted and filtered, and then the contents of Ni(II), Pb(II), and Zn(II) were determined. The amount of leached metals from the tested sorbent was calculated as follows:

$$q = \frac{Cm}{V} \tag{22}$$

where q is the amount of metal released at a solid to liquid ratio of 1:10 (mg/kg DM), C is the metal concentration in the effluent (mg/dm^3), V is the volume of the washing liquid used (dm^3), and m is the dry matter (DM) mass of the analytical sample (kg).

3. Results and Discussion

3.1. Material Characterization

3.1.1. Granulometric Analysis

The granulometric analysis (Figure 2) revealed the presence of three dominant grain classes in the tested material, namely: 0.2–6 µm, 7–16 µm, and 17–40 µm. The percentage shares of these classes were 60%, 30%, and 10%, respectively. The low content of the grain size above 20 µm was related to the presence of the small amount of non-clayey minerals in the sample, especially quartz. The dominant grain class in the Pliocene clay sample was therefore the finest fraction (<6 µm), which proves the high presence of clayey minerals.

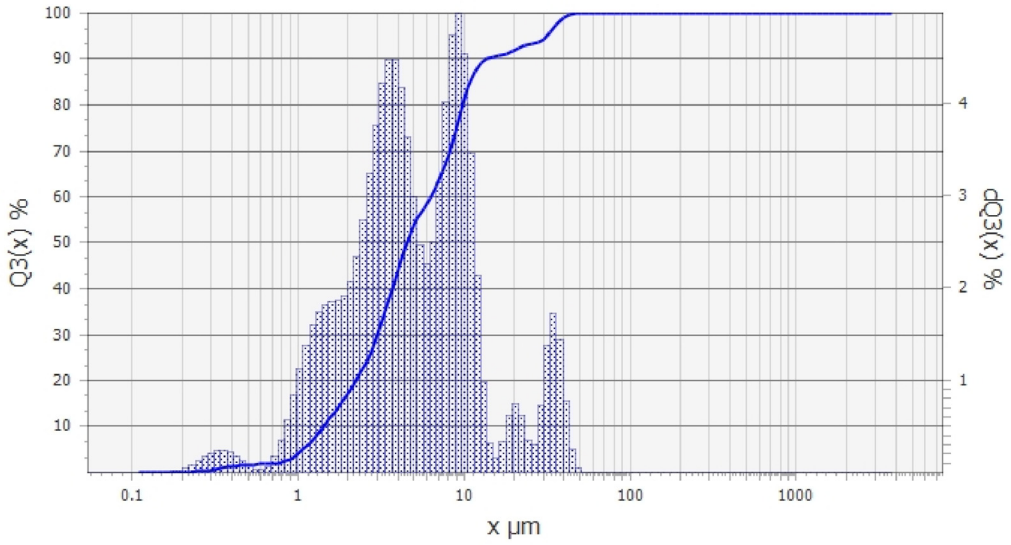


Figure 2. Granulometric analysis of the Pliocene clays used in the study.

3.1.2. Mineralogical Composition

Pliocene clays in their natural state have a gray tint. The mineralogical composition of the tested samples was determined based on XRD analysis (Figure 3), as well as DTG/TG and DTA analyses (Figures 4 and 5), respectively.

The XRD analysis showed that the main constituents of the clays were beidellite (around 45%), quartz (33%), and kaolinite (16%). The values stayed in agreement with those reported by other researchers [3]. Small amounts of illite and calcite were also found. The presence of the minerals was also confirmed with the DTG analysis. Two peaks related to weight loss were identified in the DTG curve. The total weight loss during charring was about 11%. The first peak (temperatures up to around 150 °C) reflected the dehydration process, i.e., evaporation of adsorbed water. A slight deflection on the DTG and DTA curves at a temperature of 166 °C indicated a higher amount of monovalent cations (Na^+, K^+) in the interpackage spaces, and a small amount of divalent cations (Ca^{2+}). In the temperature range of 200–350 °C, the losses in the sample mass were small. They were

most likely related to the removal of water from the hydrated iron and aluminum oxides. A strong loss of mass visible on the TG curve occurred for temperatures of 400 to 600 °C with a clear endothermic effect on the DTG curve, related to the separation of chemically bound water from clay minerals (Figure 4). The endothermic peak on the DTG curve with a maximum temperature of 501 °C was related to the thermal reactions of the beidellite decomposition, which took place at temperatures of 500–650 °C. The weight loss visible in the temperature range of 530–590 °C on the DTG curve was most likely related to the dehydroxylation of kaolinite [41]. As the kaolinite amount decreased, the dehydroxylation caused the maximums of the effects of mass loss and the maximums of endotherms to shift towards lower temperatures [42]. The shift of the endothermic maximum to a temperature of 524 °C visible on the DTA curve was confirmed by the content of this mineral in the sample. Moreover, admixtures of carbonates (calcite) were found in the analyzed sample, the thermal decomposition of which began at 600 °C on the DTA curve, with a maximum temperature of 906 °C, and it ended at 950 °C (Figure 5).

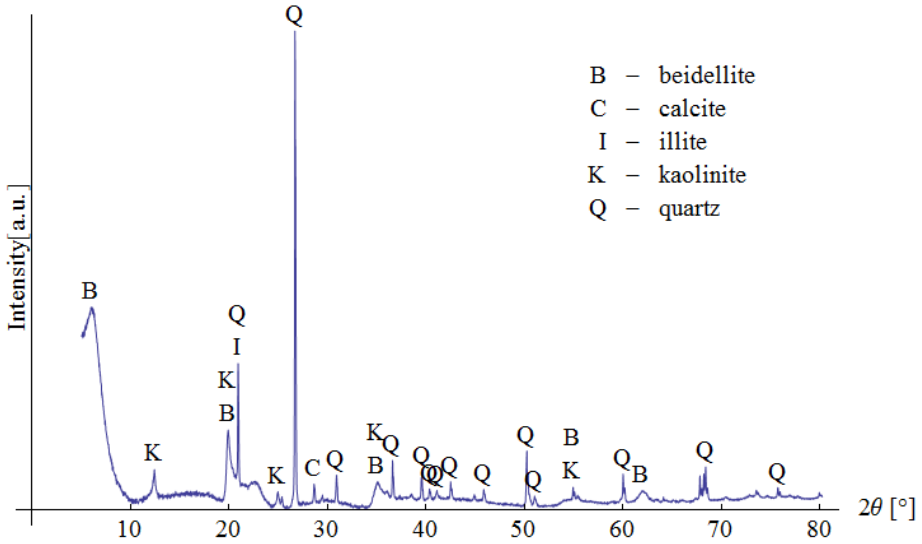


Figure 3. XRD analysis of the tested material.

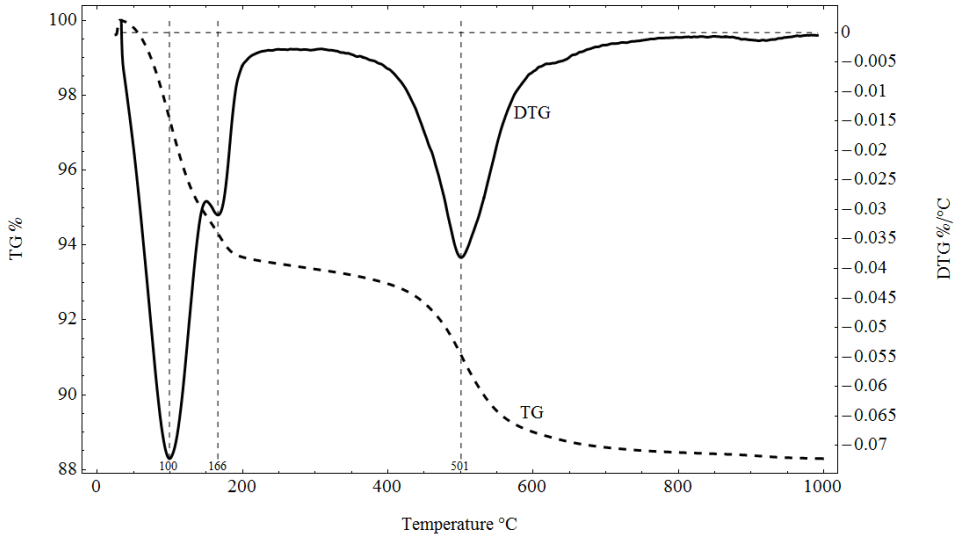


Figure 4. TG/DTG analysis results for the tested material.

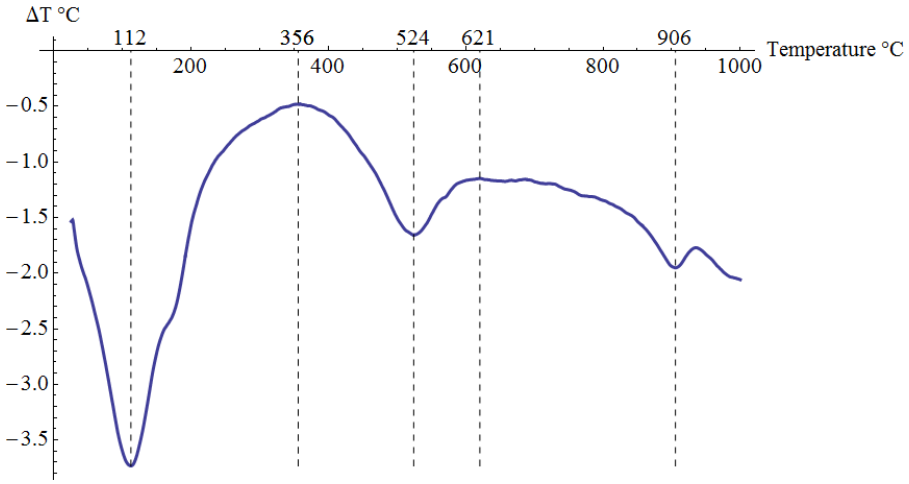


Figure 5. DTA analysis results for the tested material.

3.1.3. Chemical Composition

The chemical composition of the studied minerals reflects their mineral composition. The chemical composition of the clays showed a high content of silicon and aluminum oxides; in addition, calcium, iron, and magnesium oxides were also noticeable (Table 1). The amount of calcium oxides was higher than that of sodium oxides, which indicates the presence of the calcium type of smectites. A low Na_2O content is associated with the absence or small amounts of feldspar and mica. According to [43], SiO_2 content over 55 wt% means a good suitability, and an Al_2O_3 content from 22 wt% to 30 wt% means a good suitability for the construction of waterproofing screens. On the other hand, a low sodium content may deteriorate the waterproofing properties of beidellite clays, as the absence of this element is unfavorable from the point of view of plasticity and swelling under the influence of water [44].

Table 1. Chemical composition of the Pliocene clays studied here.

Component	SiO_2	Al_2O_3	Fe_2O_3	CaO	MgO	Cr_2O_3	MnO
Content, wt%	56.8	21.1	5.3	3.5	1.4	0.025	0.35
Component	K_2O	P_2O_5	SO_3	Na_2O	TiO_2	ZrO_2	Loss on ignition
Content, wt%	0.43	0.16	<0.01	0.45	0.27	<0.01	9.82

The content of trace elements in the tested clays and the permissible values in the soils and surface soils are presented in Table 2. The values are typical for sedimentary rocks of the Pliocene epoch. The content of trace elements in the studied material was much lower than permissible for the soils of group B, according to [45].

Table 2. The content of trace elements in the tested raw Pliocene clays and the permissible content of these metals in the soils of group B (land included in agricultural land, forest land, and wooded and shrubby land, as well as built-up and urbanized land, excluding industrial land), according to [45].

	Content, mg/kg DM								
	Ba	**Cd**	**Co**	**Cr**	**Cu**	**Ni**	**Pb**	**Sr**	**Zn**
Determined	96.17	<0.01	11.56	101.8	20.02	32.6	<0.01	64.45	123.8
Permissible	200	4	20	150	150	100	100	-	300

The tested clays were characterized by a low degree of leaching of water-soluble components (Table 3). Among the water-leaching cations, Ca^{2+}, Mg^{2+}, Na^+, and K^+ were present, while among the anions, SO_4^{2-} and Cl^- ions were present. Among the marked

heavy metal ions, the iron and strontium ions showed the greatest mobility. The concentrations of Ba, Cd, Mn, Ni, and Pb ions were below the quantification limit, while the Ag, Cr, Cu, and Zn ions were near the quantification limit. It follows that, apart from Fe and Sr ions, other heavy metal ions occur in forms hardly soluble in water. The pH of the water extract was 7.5 and also did not exceed the limit values for sewage discharged into the water and soil (Table 3).

Table 3. Composition of water extracts of the tested clays and permissible values given in [46].

	pH	Concentration, mg/dm^3							
		Ag	**Ba**	**Cd**	**Cr**	**Cu**	**Fe**	**Mn**	**Ni**
Determined	7.5	0.079	<0.01	<0.01	0.047	0.026	0.12	<0.01	<0.01
Permissible	6.5–9	0.1	2	0.4	0.5	0.5	10	-	0.5
		Concentration, mg/dm^3							
		Pb	**Sr**	**Zn**	**Mg^{2+}**	**Ca^{2+}**	**Na^{+}**	**K^{+}**	**Cl^{-}**	**SO_4^{2-}**
Determined	<0.01	0.24	0.036	5.061	26.9	3.9	6.39	<10	<15
Permissible	0.5	-	2	-	-	800	80	1000	500

3.1.4. Structural Properties

The nitrogen adsorption and desorption isotherms recorded for the tested sample are shown in Figure 6. According to the IUPAC classification, the isotherms could be classified as type IV, although there was no plateau as often encountered for isotherms of this type. The shape of the isotherm also corresponded to the type II isotherm, yet with a hysteresis loop. Type II isotherms correspond to single and multi-layer physical adsorption on porous adsorbents. Therefore, according to [47], the determined isotherm can be classified as pseudo-type II related to delayed capillary condensation. The adsorption hysteresis loop represents the H3 type characteristic of loose aggregates of planar-like particles. The calculated value of the specific surface area by the modified BET method for the tested sample was 66.1 m^2/g, and the pore volume for the tested sample was 165 mm^3/g. According to the Barrett–Joyner–Halenda method, the dominating pore diameter was 4 nm, and the average pore diameter was 15 nm.

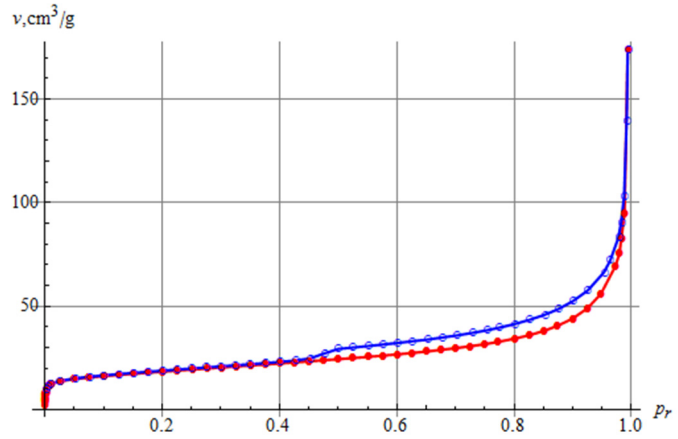


Figure 6. The N_2 adsorption and desorption isotherms for the Pliocene clays studied.

3.1.5. Point of Zero Charge pH

Figure 7 shows the pH_{pzc} results for the tested samples of Pliocene clays. The studied clays pH_{pzc} was approximately 7.1. The best adsorption of cations could be expected for $pH > pH_{pzc}$, because then the boundary between the solid and liquid phase is negative [48]. However, it should be taken into account that metal ions are precipitated for a large enough pH. In the case of Pb(II), Zn(II), and Ni(II), the precipitation occurrs for $pH \geq 5$, 6, and 7.5,

respectively [49]. When precipitation is undesirable, the adsorption should be carried out below the precipitation pH.

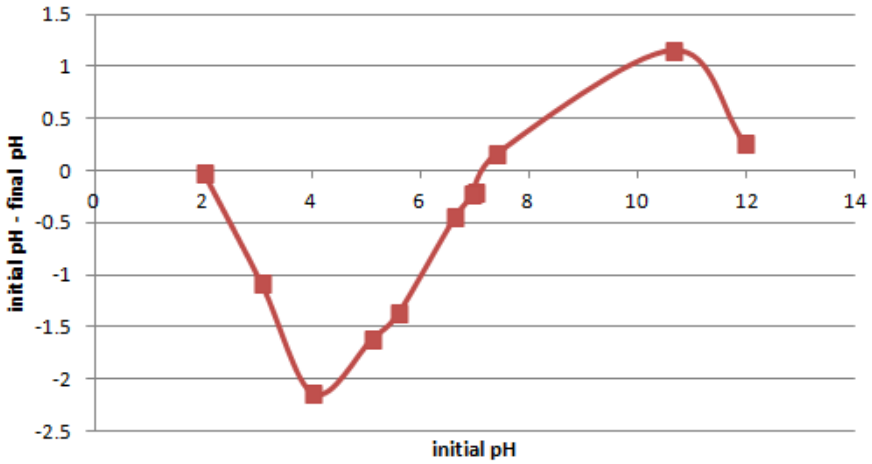


Figure 7. The pH change vs. initial pH for pH_{zpc} determination.

3.2. Optimization of Adsorption Conditions

Table 4 shows the values of coded (x_1, x_2, and x_3) and decoded (pH_0, C_0, m) values for the independent variables. Columns C_e for the three tested metals show the determined equilibrium concentrations of metal ions. Column R shows the removal percentage evaluated with Equation (2).

Table 4. CCD3 input and response data.

x_1	pH_0	x_2	C_0 [mg/dm^3]		x_3	m [g]	C_e [mg/dm^3]			Removal R [%]		
			Zn, Ni	Pb			Zn	Ni	Pb	Zn	Ni	Pb
−1	3.8	−1	26	141	−1	1.8	3.4	4.8	17.4	87.1	81.7	87.6
1	6.2	−1	26	141	−1	1.8	1.9	3.6	0.4	92.7	86.1	99.7
−1	3.8	1	74	259	−1	1.8	21.7	22.2	67.5	70.6	69.9	74.0
1	6.2	1	74	259	−1	1.8	18.3	24.1	1.9	75.1	67.4	99.3
−1	3.8	−1	26	141	1	4.2	1.7	2.5	13.0	93.4	90.6	90.7
1	6.2	−1	26	141	1	4.2	0.5	1.5	0.3	98.2	94.4	99.8
−1	3.8	1	74	259	1	4.2	8.9	13.2	42.9	88.0	82.1	83.5
1	6.2	1	74	259	1	4.2	6.3	11.0	0.5	91.4	85.1	99.8
0	5	0	50	200	0	3	6.1	7.3	10.1	87.9	85.3	95.0
0	5	0	50	200	0	3	5.8	8.2	12.2	88.5	83.6	93.9
0	5	0	50	200	0	3	5.9	7.3	10.8	88.1	85.4	94.6
−1.68	3	0	50	200	0	3	14.3	12.6	67.3	71.4	74.7	66.3
1.68	7	0	50	200	0	3	0.3	7.3	0.3	99.5	85.4	99.9
0	5	−1.68	10	100	0	3	0.2	0.7	2.5	97.9	93.1	97.5
0	5	1.68	90	300	0	3	18.1	23.0	25.0	79.9	74.5	91.7
0	5	0	50	200	−1.68	1	17.2	19.3	34.2	65.5	61.4	82.9
0	5	0	50	200	1.68	5	2.7	5.9	5.7	94.6	88.2	97.2
0	5	0	50	200	0	3	6.6	7.4	13.6	86.7	85.3	93.2
0	5	0	50	200	0	3	6.1	7.6	11.0	87.8	84.7	94.5
0	5	0	50	200	0	3	6.1	8.1	15.3	87.7	83.9	92.3

The results of the fit analysis are shown in Table 5, where the best fit coefficients a_0, a_1, . . . , a_9 for removal approximation $\widetilde{R}$, Equation (3), are given. In addition to the values of best fit parameters, the percentage variance explanation of the results is also given. The omitted coefficients were not significant in the explanation of the removal variance and lowered the adjusted R^2.

Table 5. Best fit parameters for the removal of Zn(II), Ni(II), and Pb(II) based on CCD3.

Parameter	Zn(II)		Ni(II)		Pb(II)	
i	a_i	Variance, %	a_i	Variance, %	a_i	Variance, %
0	88.1	-	84.9	-	93.8	-
1	4.81	18	1.94	4	8.72	68
2	−5.60	25	−5.84	34	−2.29	5
3	6.90	38	6.75	46	2.73	7
4	-	-	−0.97	<1	2.55	3
5	-	-	-	-	−1.50	1
6	2.74	3.5	1.60	1	-	-
7	-	-	−1.04	<1	−3.22	10
8	-	-	-	-	0.84	<1
9	−2.26	4.5	−2.89	9	−0.77	<1
Unexplained	-	11	-	5	-	5
Adjusted R^2	0.85	-	0.92	-	0.91	-

The surfaces of constant $\widetilde{R}$ for Zn(II), Ni(II) and Pb(II) are shown in Figure 8a,c,e. Although 100% is visible (magenta surfaces), it should be emphasized that $\widetilde{R}$ is just an approximation, and its values should be treated with care. Nevertheless, a general trend can be observed. It follows that the removal is the higher the larger pH_0 for all tested metals. Also larger values of adsorbent mass result in higher removal, and larger values of the initial concentrations give usually lower removal. The initial pH and adsorbent mass can be freely controlled, but the concentration of metal ions cannot be selected during normal operation—it is a result of the factual state of solution. Therefore, to obtain more representative results it is proposed to take the mean value of removal over the considered range:

$$\overline{R}(x_1, x_2) = \frac{1}{2\alpha} \int_{-\alpha}^{\alpha} \widetilde{R}(x_1, x_2, x_3) dx_2 \tag{23}$$

The $\overline{RR}$ functions for the tested metals are shown as contour plots in Figure 8b,d,f. Table 6 shows the $\overline{R}$ functions and their maxima in the considered range of variables. It follows that the optimal conditions of adsorption for the three metals are similar. Too high pH can cause precipitation of metal. Taking into account that the considerations are based on approximate expression it is suggested to take pH_0 around 4–6 and adsorbent mass around 4 g per 200 cm^3.

Table 6. The results of optimization of the adsorption conditions.

Metal	$\overline{R}$	Maximum		
		(x_1, x_3)	pH_0	m [g]
Zn(II)	$88.1 + 4.81x_1 + 6.90x_3 - 2.26x_3^2$	(1.68, 1.52)	7.0	4.8
Ni(II)	$84.9 + 1.94x_1 + 6.75x_3 - 1.04x_1^2 - 2.91x_3^2$	(0.93, 1.16)	6.1	4.4
Pb(II)	$94.6 + 8.72x_1 + 2.72x_3 - 1.50x_1x_3 - 3.22x_1^2 - 0.77x_3^2$	(1.22, 0.58)	6.4	3.7

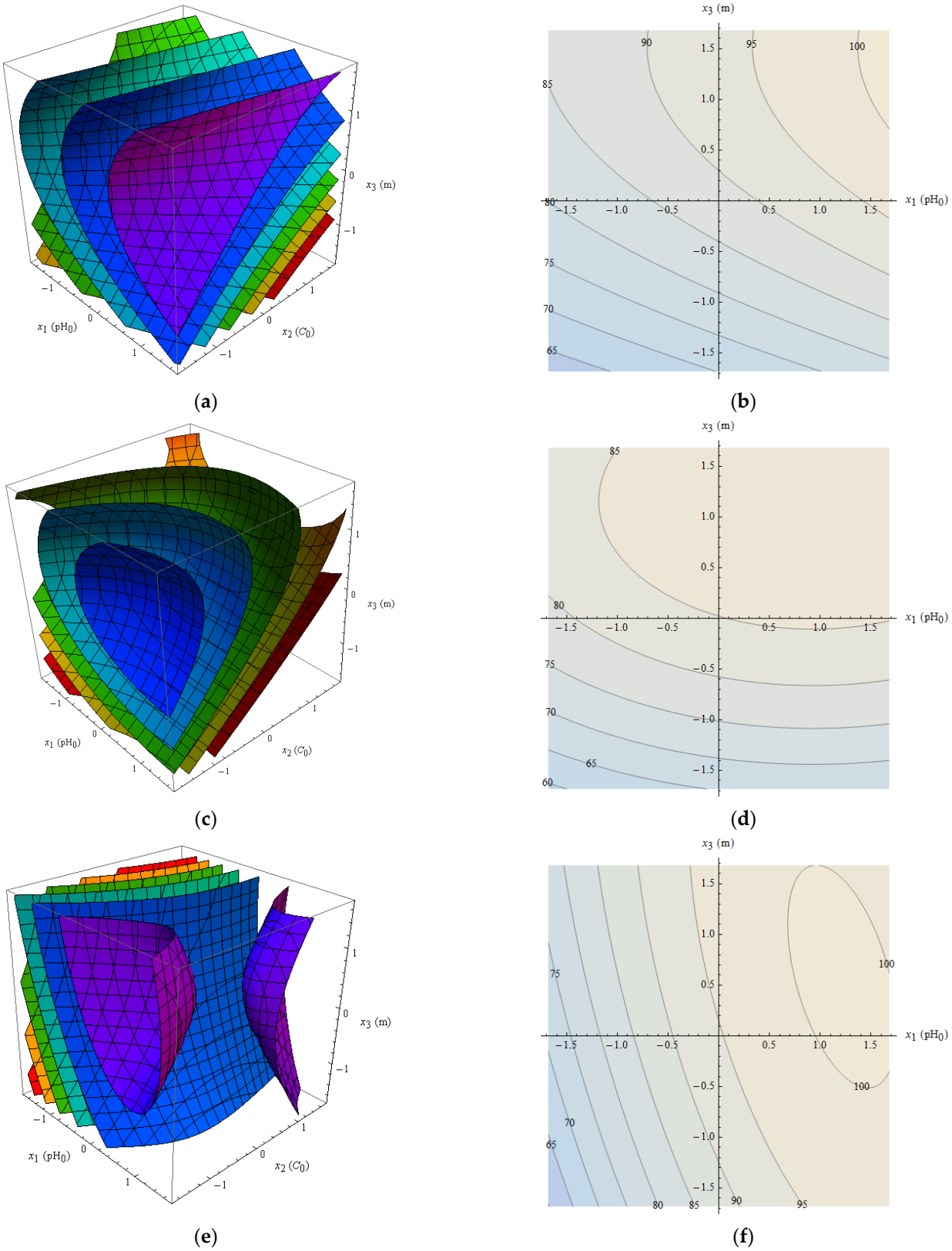


Figure 8. Graphical view of the removal approximation: surfaces of constant $\widetilde{R}$ for Zn(II) (**a**), Ni(II) (**c**), and Pb(II) (**e**), and contour plots of $\overline{R}$ for Zn(II) (**b**), Ni(II) (**d**), Pb(II) (**f**); color scale for figures a, c, e: red—75%; yellow—80%; green—85%; cyan—90%; blue—95%; magenta—100%.

3.3. Adsorption Kinetics

The results concerning the adsorption kinetics are summarized in Table 7. First of all, it can be noticed that the adsorption occurred very quickly; the half-times predicted by the PFO, PSO, and IPD1 models were in the order of a minute, and the C value in the IPD model was close to the q_e values in the other models. The PFO, PSO, and IPD1 models had similar quality of fit and similar q_e values. Although in most cases the PSO model had a slightly better fit, because of the very fast adsorption and the obtained error estimation in the coefficients of the models, it was not possible to unequivocally determine which of the models best reflected the adsorption kinetics. The IPD model given by Formula (12) was not adequate for the description of the adsorption in the considered time period because of the high value of C.

Table 7. Kinetics analysis results (bold values for S and χ^2 indicate the best fit).

Parameter or Indicator	Unit	Ni(II)		Pb(II)		Zn(II)	
		C_0=100 mg/dm^3	C_0=200 mg/dm^3	C_0=100 mg/dm^3	C_0=200 mg/dm^3	C_0=100 mg/dm^3	C_0=200 mg/dm^3
		PFO, Equations (1)–(4)					
q_e	mg/g	6.45 ± 0.07	9.98 ± 0.07	9.74 ± 0.06	18.54 ± 0.10	6.59 ± 0.04	9.92 ± 0.15
k_1	min^{-1}	0.58 ± 0.11	0.45 ± 0.04	0.64 ± 0.09	0.68 ± 0.09	0.65 ± 0.09	0.45 ± 0.08
$t_{1/2}$	min	1.19 ± 0.22	1.53 ± 0.12	1.09 ± 0.15	1.02 ± 0.14	1.07 ± 0.16	1.55 ± 0.27
S	mg/g	0.20	0.20	0.18	0.30	0.13	0.42
χ^2	mg/g	0.031	0.019	0.017	0.025	0.012	0.091
		PSO, Equations (5)–(8)					
q_e	mg/g	6.51 ± 0.07	10.1 ± 0.05	9.77 ± 0.08	18.65 ± 0.08	6.60 ± 0.06	10.07 ± 0.13
k_2	g/(mg min)	0.43 ± 0.20	0.15 ± 0.02	0.55 ± 0.35	0.22 ± 0.06	0.92 ± 0.67	0.13 ± 0.04
$t_{1/2}$	min	0.35 ± 0.15	0.64 ± 0.07	0.19 ± 0.11	0.24 ± 0.06	0.16 ± 0.12	0.73 ± 0.21
S	mg/g	0.18	0.12	0.21	0.21	0.14	0.33
χ^2	mg/g	0.024	0.0071	0.022	0.012	0.016	0.056
		IPD, Equation (10)					
k_i	mg/g min$^{-0.5}$	0.025 ± 0.010	0.045 ± 0.021	0.0036 ± 0.014	0.045 ± 0.014	0 ± 0.010	0.078 ± 0.015
C	mg/g	6.17 ± 0.11	9.41 ± 0.23	9.66 ± 0.16	18.03 ± 0.16	6.56 ± 0.11	9.2 ± 0.17
S	mg/g	0.18	0.35	0.25	0.25	0.17	0.26
χ^2	mg/g	0.024	0.065	0.032	0.017	0.021	0.036
		IPD1, Equations (12)–(15)					
q_e	mg/g	6.47 ± 0.07	9.98 ± 0.07	9.74 ± 0.06	18.55 ± 0.10	6.59 ± 0.04	9.93 ± 0.15
B	min^{-1}	0.48 ± 0.11	0.35 ± 0.03	0.54 ± 0.09	0.58 ± 0.09	0.55 ± 0.09	0.34 ± 0.08
$t_{1/2}$	min	0.61 ± 0.14	0.85 ± 0.08	0.55 ± 0.09	0.51 ± 0.08	0.54 ± 0.09	0.86 ± 0.19
S	mg/g	0.20	0.19	0.18	0.30	0.13	0.42
χ^2	mg/g	0.031	0.018	0.017	0.024	0.012	0.089
D	μm^2/min	0.60	0.43	0.67	0.72	0.68	0.43

Using Figure 2 and assuming that the dominating adsorbent particle size r was around 3.5 μm, it was possible to estimate the equivalent diffusion coefficient D (last row in Table 7) using Equation (16). The obtained D values were similar and fell within the range of 0.43 to 0.72 μm^2/min (due to the estimated value of r, the estimation error for D was not given).

3.4. Thermodynamic Studies

The results of the analysis are shown in Table 8 and Figure 9. In each case, the enthalpy change was positive, which indicates the adsorption was an endothermic reaction. In the case of Zn(II) adsorption, the R^2 value was very small. This could be a result of several factors. First, Equation (19) assumes a constant value for ΔH, which does not necessarily take place. Second, Equation (19) is correct, but ΔH is really low, so the measurement uncertainty influences the linear relationship badly. The confirmation of a poor fit is also given by the fact that the enthalpy change is very small and the standard error of the change is larger than the change itself. This means that the value of ΔH can be positive as well as negative. Nevertheless, according to Equation (21), its influence on the free

Gibbs energy is small. The negative Gibbs free energy indicates that the adsorption was spontaneous and thermodynamically favored.

Table 8. The thermodynamic studies' results for the Pb(II), Ni(II), and Zn(II) adsorption (the initial concentration was 100 mg/dm^3).

Temperature, T [°C]	Equilibrium Concentration (C_e) [mg/dm3]			The Gibbs Free Energy (ΔG) [kJ/mol]		
	Pb(II)	Ni(II)	Zn(II)	Pb(II)	Ni(II)	Zn(II)
20	5.06	36.4	33.2	−19.7	−15.4	−15.6
30	4.34	32.9	32.1	−21.1	−16.2	−16.1
40	3.52	28.2	34.0	−22.4	−16.9	−16.7
50	2.40	28.1	32.1	−23.7	−17.7	−17.2
ΔH [kJ/mol]	19.4 ± 3.3	7.4 ± 1.6	0.3 ± 1.2			
ΔS [J/(mol K)]	134 ± 11	77.0 ± 5.1	54.4 ± 3.9			
R^2	0.943	0.918	0.038			

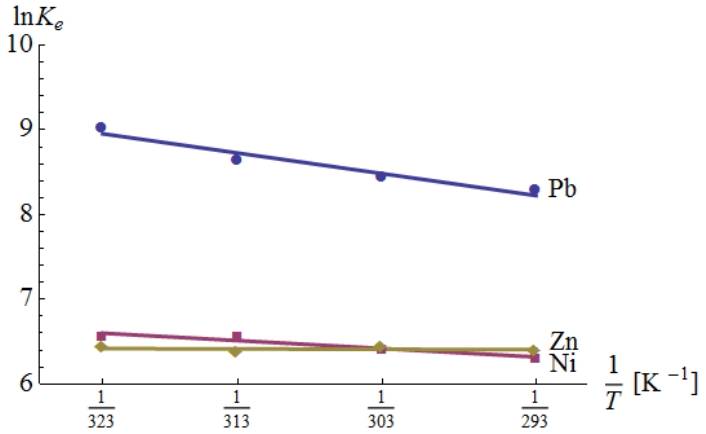


Figure 9. The Van't Hoff plots for Pb(II), Ni(II) and Zn(II) adsorption.

3.5. Leaching Studies

The process of leaching toxic elements, such as Pb, Ni, and Zn, from mineral waste has a significant impact on the water and soil environment of the areas where the waste is deposited. The results of the leaching analysis after the sorption process are summarized in Table 9.

Table 9. Results of leaching of Pb(II), Ni(II), and Zn(II) from Pliocene clays after sorption.

Metal	Mean Concentration in the Effluent, mg/dm^3	Standard Deviation, mg/dm^3	Relative Standard Deviation, %	Effluent pH	Leachabilty, mg/kg DM	Percentage Leachability, %	Permissible Leachability, mg/kg DM *		
							A	B	C
Pb	0.077	0.003	3.92	7.09	0.77	0.02	0.5	10	50
Ni	0.454	0.002	0.44	7.15	4.54	0.14	0.4	10	40
Zn	0.232	0.021	9.19	6.89	2.32	0.05	4	50	200

* Leaching limits specified in [50]: landfill for inert waste (A), other than inert and hazardous (B), and hazardous (C).

The contents obtained from the metals leached from the Pliocene clays were compared with the permissible values used in the classification and acceptance of waste for a storage in landfills of a given type, included in [50]. The criteria related to three categories of waste and their corresponding landfill types: inert (A), other than inert and hazardous (B), and hazardous (C). The tested adsorbent met the requirements for waste and its storage in an inert waste landfill (A) in terms of Zn sorption (2.32 < 4). The amount of Pb washed out (0.77 mg/kg DM) slightly exceeded the value permissible for landfills of inert waste (0.5 mg/kg DM). This shows that the potential impact on the environment was relatively

low. In the case of nickel leaching, the requirements for waste and its storage in landfills other than hazardous and inert (B) were met (4.54 < 10). Among the examined heavy metal ions, nickel was the most mobile because of its susceptibility to bonding with organic substances, to a large extent in the form of mobile chelates even under the conditions of neutral or alkaline reactions [11]. However, the tests were carried out at a relatively high initial concentrations of the metals (100 mg/dm^3), which resulted in a rather high accumulation in the adsorbent, which could cause an increase in leachability.

Considering the absolute values of leachability of the adsorbed metal ions, they could be arranged in the following order: Ni > Zn > Pb. The low leachability of Pb observed in the water extracts may have been related to the limited availability of this element resulting from strong interactions between clay minerals, organic matter, or secondary forms of iron or manganese. It is also possible to form poorly soluble secondary mineral compounds in combination with sulfates, carbonates, hydroxycarbonates, or phosphates [51,52].

The obtained concentrations of Pb, Ni, and Zn in water extracts were also compared with the permissible values in wastewater [46], as shown in Table 3. The contents of Pb, Ni, and Zn, as well as the pH of the water extract, did not exceed the permissible values for sewage discharged into the water and soil. A low percentage of leaching (below 0.2%) proved their negligible susceptibility against leaching from Pliocene clays through their interactions with aqueous solutions.

4. Conclusions

Based on the results obtained, the following conclusions can be formulated:

- The chemical composition of the studied rocks allows for their use in the adsorption process without the risk of secondary contamination of the treated waters or sewage.
- Structural parameters, such as the specific surface area and the dominant pore size, indicate the potentially good sorption properties of the studied rocks.
- The pH_{pzc} = 7.1 allows for the adsorption to be carried out in a nearly neutral pH.
- The optimization of the selection of adsorption conditions indicates that the optimal dose of the adsorbent is about 20 g/dm^3, and the pH value should be about 6, which is consistent with the conclusions regarding the point of zero charge pH. The pH value may be lowered to avoid precipitation if necessary; however, this may weaken the adsorption.
- The results of the research on kinetics show that the adsorption process is very fast; after just a few minutes, the adsorbent is practically saturated with metal ions.
- The negative Gibbs free energy indicates that the adsorption is spontaneous and thermodynamically favored.
- The low leachability of the Pb, Zn, and Ni from the tested clays, weakly alkaline pH, and high ability to bind metal cations make the post-mine Pliocene clay waste a low-cost effective sorbent for Pb(II), Ni(II), and Zn(II) ions.

Funding: This work was financially supported by the Faculty of Infrastructure and Environment of the Czestochowa University of Technology.

Data Availability Statement: The data presented in this study are available on request from the corresponding author.

Conflicts of Interest: The author declares no conflict of interest.

References

1. Central Statistical Office. Environmental Protection. Available online: https://stat.gov.pl/obszary-tematyczne/srodowisko-energia/srodowisko/ochrona-srodowiska-2020,1,21.html (accessed on 1 February 2021).
2. Ratajczak, T.; Bahranowski, K.; Górniak, K.; Szydłak, T.; Wyszomirski, P. Kopaliny towarzyszące. In *Eksploatacja Selektywna Węgla Brunatnego i Kopalin Towarzyszących Wraz z Uwarunkowaniami Techniczno-Ekonomicznymi i Korzyściami Ekologicznymi*; Stryszewski, M., Ed.; Wydawnictwo CPPGSMiE PAN: Krakow, Poland, 1995; pp. 45–74.
3. Ratajczak, T.; Hycnar, E. *Kopaliny Towarzyszące w Złożach Węgla Brunatnego. Geologiczno-Surowcowe Aspekty Zagospodarowania Kopalin Towarzyszących, Tom 1*; Wydawnictwo IGSMiE PAN: Krakow, Poland, 2017.

4. Chudek, M.; Hycnar, J.; Janiczek, S.; Plewa, F. *Węgiel Brunatny, Utylizacja Surowców Towarzyszących i Odpadów Elektrownianych*; Wydawnictwo Politechniki Śląskiej: Gliwice, Poland, 1999.
5. Ratajczak, T.; Hycnar, E.; Bożęcki, P. *Kryterium Mineralogiczne Jako Element Oceny Przydatności Niektórych Polskich Surowców Ilastych do Budowy Przesłon Hydroizolacyjnych*; Studia, Rozprawy, Monografie 194; Wydawnictwo IGSMiE PAN: Krakow, Poland, 2015; pp. 1–164.
6. Sałaciński, R.; Gąsiński, A. Możliwości wykorzystania gospodarczego surowców ilastych z plioceńskich iłów z KWK Bełchatów—Pole Szczerców. *Górnictwo Odkryw.* **2012**, *1–2*, 83–89.
7. Kyzioł-Komosińska, J.; Rosik-Dulewska, C.; Kocela, A. Sorption properties and applicability of neogene clays in removal of heavy metal ions from wastewater. *Przem. Chem.* **2008**, *87*, 501–505.
8. Kyzioł-Komosińska, J.; Kukułka, L. *Wykorzystanie Kopalin Towarzyszących Pokładom Złóż Węgli Brunatnych do Usuwania Metali Ciężkich z Wód i Ścieków*; Insytut Podstaw Inżynierii Środowiska Polskiej Akademii Nauk: Zabrze, Poland, 2008.
9. Jabłońska, B.; Busch, M.; Kityk, A.V.; Huber, P. Natural and chemically modified post-mining clays—Structural and surface properties and preliminary tests on copper sorption. *Minerals* **2019**, *9*, 704. [CrossRef]
10. Briffa, J.; Sinagra, E.; Blundell, R. Heavy metal pollution in the environment and their toxicological effects on humans. *Heliyon* **2020**, *6*, e04691. [CrossRef] [PubMed]
11. Kabata-Pendias, A.; Pendias, H. *Biochemia Pierwiastków Śladowych*; Wydawnictwo Naukowe PWN: Warsaw, Poland, 1999.
12. Bislimi, K.; Halili, J.; Sahiti, H.; Bici, M.; Mazreku, I. Effect of mining activity in accumulation of heavy metals in soil and plant (*Urtica dioica* L.). *J. Ecol. Eng.* **2021**, *22*, 1–7. [CrossRef]
13. Usman, K.; Al-Ghouti, M.A.; Abu-Dieyeh, M.H. The assessment of cadmium, chromium, copper, and nickel tolerance and bioaccumulation by shrub plant *Tetraena qataranse*. *Sci. Rep.* **2019**, *9*, 5658. [CrossRef] [PubMed]
14. Migaszewski, Z.M.; Gałuszka, A. *Podstawy Geochemii Środowiska*; Wydawnictwo Naukowo-Techechniczne: Warsaw, Poland, 2007.
15. Kopcewicz, J.; Lewak, S. *Fizjologia Roślin*; Wydawnictwo Naukowe PWN: Warsaw, Poland, 2002.
16. Ali, H.; Khan, E.; Ilahi, I. Environmental chemistry and ecotoxicology of hazardous heavy metals: Environmental persistence, toxicity, and bioaccumulation. *J. Chem.* **2019**, *2019*, 6730305. [CrossRef]
17. Kim, T.; Kim, S.; Tak, H.; Kim, K.; Chung, C.-W.; Lee, M. Mechanisms at different pH for stabilization of arsenic in mine tailings using steelmaking slag. *Minerals* **2020**, *10*, 900. [CrossRef]
18. Wei, W.; Ma, R.; Sun, Z.; Zhou, A.; Bu, J.; Long, X.; Liu, Y. Effects of mining activities on the release of heavy metals (HMs) in a typical mountain headwater region, the Qinghai-Tibet Plateau in China. *Int. J. Environ. Res. Public Health* **2018**, *15*, 1987. [CrossRef]
19. Stefanowicz, A.M.; Woch, M.W.; Kapusta, P. Inconspicuous waste heaps left by historical Zn–Pb mining are hot spots of soil contamination. *Geoderma* **2014**, *235–236*, 1–8. [CrossRef]
20. Janas, M.; Zawadzka, A. Wpływ składowiska odpadów przemysłowych na środowisko. *Ecol. Eng.* **2017**, *18*, 64–73. [CrossRef]
21. Leita, L.; Enne, G.; Nobili, M.D.; Baldini, M.; Sequi, P. Heavy metal bioaccumulation in lamb and sheep bred in smelting and mining areas of S. W. Sardinia (Italy). *Environ. Contam. Toxicol.* **1991**, *446*, 887–893. [CrossRef] [PubMed]
22. Zhang, X.; Yang, L.; Li, Y.; Li, H.; Wang, W.; Ye, B. Impacts of lead/zinc mining and smelting on the environment and human health in China. *Environ. Monit. Assess.* **2012**, *184*, 2261–2273. [CrossRef] [PubMed]
23. Zhang, J.H.; Xu, Y.N.; Wu, Y.G.; Hu, S.H.; Zhang, Y.J. Dynamic characteristics of heavy metal accumulation in the farmland soil over Xiaoqinling gold-mining region Shaanxi China. *Environ. Earth Sci.* **2019**, *78*, 25. [CrossRef]
24. Kowalska, M.; Mikulski, S.Z.; Sidorczuk, M. *Cynk, Ołów*; Państwowa Służba Geologiczna o Surowcach Mineralnych Polski; Państwowy Instytut Geologiczny—Państwowy Instytut Badawczy: Warsaw, Poland, 2020. Available online: https://www.pgi.gov.pl/dokumenty-pig-pib-all/foldery-instytutowe/foldery-surowcowe-2018/6216-folder-cynk-i-olow/file.html (accessed on 19 January 2021).
25. U.S. Geological Survey. Mineral Commodity Summaries. 2021. Available online: https://www.usgs.gov/centers/nmic/mineral-commodity-summaries (accessed on 5 May 2021).
26. Malon, A.; Tymiński, M.; Mikulski, S.Z.; Oszczepalski, S. Surowce metaliczne. In *Bilans Zasobów Złóż Kopalin w Polsce wg Stanu na 31.12.2019 r.*; Szuflicki, M., Malon, A., Tymiński, M., Eds.; Państwowy Instytut Geologiczny—Państwowy Instytut Badawczy: Warsaw, Poland, 2020; pp. 52–67. Available online: http://cima.ibs.pw.edu.pl/wp-content/uploads/bilans_2019.pdf (accessed on 19 January 2021).
27. San-Pedro, L.; Méndez-Novelo, R.; Hernández-Núñez, E.; Flota-Bañuelos, M.; Medina, J.; Giacomán-Vallejos, G. Selection of the activated carbon type for the treatment of landfill leachate by fenton-adsorption process. *Molecules* **2020**, *25*, 3023. [CrossRef] [PubMed]
28. De Abreu Domingos, R.; da Fonseca, F.V. Evaluation of adsorbent and ion exchange resins for removal of organic matter from petroleum refinery wastewaters aiming to increase water reuse. *J. Environ. Manag.* **2018**, *214*, 362–369. [CrossRef]
29. Hosseini Hashemi, M.S.; Eslami, F.; Karimzadeh, R. Organic contaminants removal from industrial wastewater by CTAB treated synthetic zeolite Y. *J. Environ. Manag.* **2019**, *233*, 785–792. [CrossRef]
30. Jabłońska, B.; Kityk, A.V.; Busch, M.; Huber, P. The structural and surface properties of natural and modified coal gangue. *J. Environ. Manag.* **2017**, *190*, 80–90. [CrossRef]
31. Jabłońska, B.; Siedlecka, E. Removing heavy metals from wastewaters with use of shales accompanying the coal beds. *J. Environ. Manag.* **2015**, *155*, 58–66. [CrossRef]

32. Jabłońska, B. Removing of Cr(III) and Cr(VI) compounds from aqueous solutions by shale waste rocks. *Desalination Water Treat.* **2020**, *186*, 234–246. [CrossRef]
33. Bajda, T. Sorbenty w oczyszczaniu ścieków. *Przegląd Komunal.* **2017**, *7*, 44–46.
34. Taha, Y.; Benzaazoua, M.; Hakkou, R.; Mansori, M. Coal mine wastes recycling for coal recovery and eco-friendly bricks production. *Miner. Eng.* **2017**, *107*, 123–138. [CrossRef]
35. Szamałek, K.; Speczik, S. Możliwości zastosowania krajowych surowców ilastych do utylizacji odpadów galwanicznych. *Ceram. Pol. Biul. Ceram.* **1994**, *446*, 341–346.
36. Polish Std. PN-EN ISO 12677:2011. *Analiza Chemiczna Wyrobów Ogniotrwałych Techniką Fluorescencji (XRF)—Metoda Perły*; Wydawnictwa Normalizacyjne: Warsaw, Poland, 2011.
37. Skalmowski, K.; Wolska, K.; Pieniak, U.; Roszczyńska, I. *Badania Właściwości Technologicznych Odpadów Komunalnych. Ćwiczenia Laboratoryjne*; Wydawnictwo Oficyna Wydawnicza Politechniki Warszawskiej: Warsaw, Poland, 2004; pp. 94–97.
38. Polish Std. PN-EN 12457-4:2006. *Charakteryzowanie Odpadów. Wymywanie. Badanie Zgodności w Odniesieniu do Wymywania Ziarnistych Materiałów Odpadowych i Osadów*; Wydawnictwa Normalizacyjne: Warsaw, Poland, 2006.
39. Tripathy, S.S.; Kanungo, S.B. Adsorption of Co^{2+}, Ni^{2+}, Cu^{2+} and Zn^{2+} from 0.5 M NaCl and major ion sea water on amixture of δ-MnO_2 and amorphous FeOOH. *J. Colloid Interface Sci.* **2005**, *284*, 30–38. [CrossRef]
40. Ho, Y.S.; Ng, J.C.Y.; McKay, G. Kinetics of pollutant sorption by biosorbents: Review. *Sep. Purif. Rev.* **2000**, *29*, 189–232. [CrossRef]
41. Földvari, M. *Handbook of Thermogravimetric System of Minerals and Its Use in Geological Practice*; Occasional Papers of the Geological Institute of Hungary: Budapest, Hungary, 2011; p. 63.
42. Wyrwicki, R. *Analiza Derywatograficzna Skał Ilastych*; Wydawnictwo Uniwersytetu Warszawskiego: Warsaw, Poland, 1988.
43. Technical Approval. *Aprobata Techniczna IMUZ/18-0011-00 do Stosowania w Budownictwie Melioracyjnym Roztworu Hydroizolującego na Bazie Glin Polimineralnych*; Instytut Melioracji Użytków Zielonych: Falenty, Poland, 2002.
44. Panna, W.; Wyszomirski, P.; Motyka, J. Możliwości wykorzystania wybranych surowców smektytowych jako materiałów dla celów hydroizolacyjnych. *Zesz. Nauk. Inst. GSMiE PAN* **2012**, *83*, 131–145.
45. Regulation of the Minister of Environment of 9 September 2002 on soil quality standards and land quality standards. *Dz.Ustaw* **2002**, *165*, 1359. (In Polish)
46. Regulation of the Minister of Environment of 18 November 2014 on the conditions to be met when discharging sewage into water or soil, and on substances particularly harmful to the aquatic environment. *Dz. Ustaw* **2014**, *1800*. (In Polish)
47. Sing, K.S.W.; Everett, D.H.; Haul, R.A.W.; Moscou, L.; Pierotti, R.A.; Rouquerol, J.; Siemieniewska, T. Reporting physisorption data for gas/solid systems with Special Reference to the Determination of Surface Area and Porosity, International union of pure and applied Chemistry physical chemistry division commission on colloid and surface chemistry including catalysis. *Pure Appl. Chem.* **1985**, *57*, 603–619.
48. Appel, C.; Ma, L.Q.; Rhue, R.D.; Kennelley, E. Point of zero charge determination in soils and minerals via traditional methods and detection of electroacoustic mobility. *Geoderma* **2003**, *113*, 77–93. [CrossRef]
49. Kowal, A.L.; Świderska-Bróż, M. *Oczyszczanie Wody*; Wydawnictwo Naukowe PWN: Warsaw, Poland, 1996.
50. Regulation of the Minister of Economy of 16 July 2015 on the criteria and procedures for allowing waste to be deposited at a given type of landfill. *Dz. Ustaw* **2015**, *1277*. (In Polish)
51. Harrell, J.A.; Belsito, M.E.; Kumar, A. Radon hazards associated with outcrops of Ohio Shale in Ohio. *Environ. Geol. Water Sci.* **1991**, *18*, 17–26. [CrossRef]
52. Piszcz-Karaś, K.; Łuczak, J.; Hupka, J. Wpływ pH na ługowanie zwiercin łupkowych roztworami wodnymi. In *Łupek Miedzionośny III*; Kowalczuk, P.B., Drzymała, J., Eds.; WGGG PWr: Warsaw, Poland, 2017; pp. 78–96. [CrossRef]